Roskilde University

The Effect of Anti-Freeze Proteins on Water-Rich Glycerol-Water Mixtures

Authors
Jonatan Heine Langer
William Fatum Stockner
Wesley Allen Paskett

Supervisor
Jan Gabriel

May 24, 2022

Abstract

The effects of antifreeze proteins (AFPs) on the freezing temperatures of water is well studied and known today. Studies of the affects of antifreeze proteins on glass transition and melting temperatures have been conducted on samples containing relatively high concentrations of glycerol and water. In this paper we conduct experiments with antifreeze proteins in water-dominated glycerol/water mixtures to determine how AFPs affect the glass transition and melting temperatures of these samples.

We present the theory behind the various interactions that occur between components of the various mixtures studied and provide mathematical background and proofs to verify our methods. We discuss the hardware and software setups, experimental procedure, preparation of samples and analysis of the gathered data.

Our analysis of a 23% glycerol/water mixture with varying concentrations of teleost type III antifreeze proteins determined that there was a lowering of the glass transition temperature by 11.32 K at a peak concentration of 1 $mMol$ antifreeze protein. We also conducted preliminary tests with pure mixtures and those this added buffer, added buffer + BSA protein and buffer + insect AFP. The experimental results obtained from the raw data is presented as well as information on how the data was interpreted. Uncertainties, arbitrary choices and areas of future research are established for suggestions of the continued research of these phenomena.

Contents

1 Introduction

"In this universe, there's only one absolute... everything freezes!"
- *Mr Freeze*, Batman & Robin (1997) [1].

It would have been more accurate to say that there is one absolute... zero Kelvin. As materials approach this temperature, the individual molecules comprising them become static. At sufficiently low temperatures materials will show physical changes, for example the crystalization of liquid water to form solid ice at 273.15 K [2]. It has been shown that at fast enough cooling rates, in certain materials, the physical change becomes different, as the material does not have time to organize into crystal structures and is effectively frozen in place. Such a material is called a glass [3, 4].
Shown in *Antifreeze Proteins* [5] by Ramløv (2020), certain proteins have anti-freezing properties, however do not fully prevent freezing from occurring at sufficiently low temperatures. Interestingly, certain mixtures of glycerol and water also affect the temperatures at which a material transitions to and from a solid. The melting temperatures of these materials have been studied by Lane [2], and the glass transition temperatures have been studied previously [4, 6–9] for mixtures above a 28% molar glycerol concentration $x_{\text{gly}} = 0.28$. This point is referred to in the literature as the eutectic point [2]. Additionally, investigation into the effects of anti-freeze proteins (AFPs) have been studied above the eutectic point [10]. However, the glass transition temperature below the eutectic point of glycerol water, i.e. for water-rich compositions, has not been investigated thoroughly. Similarily, the effect of AFPs in these concentrations lack significant study.

1.1 Research Question and Project Aim

It is the goal of this report to build upon previous research by exploring and answering the following research question:

How do anti-freeze proteins affect the solid-liquid phase transition temperatures in water-rich compositions of glycerol-water mixtures?

To answer this research question this report will present theoretical knowledge relevant to the chemical, physical, and biological aspects of this investigation. This knowledge will serve as a foundation to understand the rest of the report.
Using a method known as thermalization calorimetry developed at Roskilde University [4], this report will study the temperatures at which different mixtures transition between glass, crystal and liquid states. In particular we investigate the behavior of the glass transition temperature (T_{g}) and the melting temperature (T_{M}) of glycerol-water mixtures, both of which this method allows us to extract for a variety of mixture samples. A comparison of the temperatures will represent the effect of a particular treatment process. The investigated processes include the addition of buffer ions and proteins, with and without reported anti-freeze properties. We also investigate the effect of varying the concentration of AFP solute in a mixture of constant molar composition.
This report will discuss some of the variability in the presented data and address possible uncertainties. It will also discuss further research that can be done regarding the material properties of anti-freeze protein mixtures, such as ours. The report will conclude by answering the research question of our problem formulation.

2 Theory

This section aims to briefly describe the theoretical concepts appearing throughout the report. First we introduce the chemical principles relevant to the understanding of the problem. Here we look at the hydrogen-bond formations created during supercooling of glycerol and water molecules.
In subsection 2.2 we provide an explanation of the thermodynamic principles that allow for thermalization calorimetry measurements, the method of which will be elaborated on in subsection 3.1. This section will also described solid-liquid phase transitions and the definition of glass.
Additionally, we provide a basic description of anti-freeze proteins in subsection 2.3.

2.1 Chemistry Preliminaries

Glycerol and water mixtures will be the base mixture we will be using for tests due to its cryprotectant and glass-transition properties. The importance of glycerol is its ability to stabilize macromolecules like proteins during experiments below the freezing point of water $T < 273.15$ K, such an experiment is called a cryogenic experiment [11]. Glycerol does not crystallize, but when cooled to cryogenic temperatures forms a glass, as described in section 2.2.3. Combining glycerol with water allows for their mixture to freeze into a glass-like structure at cryogenic temperatures. The leading hypothesis among scientists is that this behavior is due to the formation of extended hydrogen-bond networks between water and glycerol molecules, effectively altering the native structure of pure water. Pure water assembles into a crystalline structure upon cooling below freezing temperatures as shown in figure 1.a. The addition of glycerol changes the arrangement of water molecules in the bulk solution (figure 1.b), preventing the formation of large, organized ice crystals.

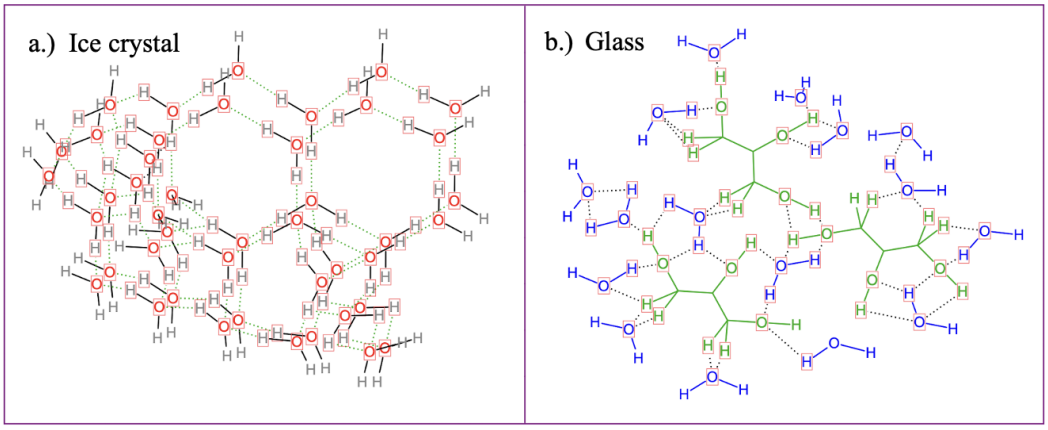

Figure 1: **a.)** Depiction of the ordered fashion in which water molecules arrange themselves when their degrees of freedom are frozen into place by sufficient cooling. Note: This is a two dimensional representation, however, this is meant to represent a three dimensional distribution of molecules. **b.)** Depiction of the hydrogen-bonding that occurs among individual water and glycerol molecules in solution. Glycerol molecules also form hydrogen bonds with other glycerol molecules, creating a hydrogen-bonded network of water and glycerol.

Varying mixtures of glycerol and water have been tested and shown to produce microsegregated regions of water-rich and glycerol-rich densities. Microsegregation here refers to water molecules tending towards other water molecules and glycerol molecules to other glycerol molecules, all while maintaining the homogeneity of the solution. This microsegregation forms a matrix between the water and glycerol molecules, effectively encapsulating the water and therefore inhibiting the formation of large crystals. This also produces the desired glassy state [11]. This is why glycerol-water mixtures are popular as a cryoprotectant in low-temperature studies of proteins [12], and why we will be using it for the purposes of studying the effects of AFPs on glass transition, described in section 2.2.3.

2.2 Thermodynamics

In this section we will give an overview of solid-liquid phase transitions, with the goal of understanding these processes in mixtures. We also provide a brief description of glassy materials and the conditions

that allow for a system to enter an amorphous phase.
Much of the experimental work covered in this report is built on our understanding of heat. Heat is a transfer of microscopic kinetic energy [13, 14]. A substance in a stable phase will change temperature at a rate given by its heat capacity C, given by

$$C = \frac{\mathrm{d}Q}{\mathrm{d}T}. \tag{1}$$

We will utilize this definition in section 3.1. Additionally, we introduce the thermodynamic identity [13]. The thermodynamic identity is fundamentally a statement about the change in entropy of a system with respect to its thermodynamic properties. For example, if the internal energy of a system changes by $\mathrm{d}\,U$ and the volume by $\mathrm{d}\,V$, the identity states that the entropy change $\mathrm{d}S$ is

$$\mathrm{d}S = \frac{1}{T}\mathrm{d}U + \frac{P}{T}\mathrm{d}V, \tag{2}$$

where P is the pressure and T the temperature of the system. At constant volume this is in fact the definition of temperature $\frac{1}{T} \equiv \left(\frac{\partial S}{\partial U}\right)_V$ [13]. We will now look into some specifics of the solid-liquid phase transition of substances.

2.2.1 Melting

Melting refers to the phase transition of a substance from a solid substance to a liquid. The stable phase of a given substance is determined by its Gibbs free energy, G; where the phase with the least free energy is the most stable [13]. For instance, ice, the solid form of H_2O, has less free energy than liquid water at temperatures $T < 0$ °C and atmospheric pressure $P = 1$ atm, thus ice forms from water upon sufficient cooling. To understand this we look closer at the Gibbs free energy of a system, given by

$$G = U - TS + PV, \tag{3}$$

where U is the internal energy of the system, V its volume, and S its entropy [13]. From the thermodynamic identity (2) combined with equation (3) we find that a small change in the free energy $\mathrm{d}\,G$ is given by

$$\begin{aligned} \mathrm{d}G &= \mathrm{d}U - \mathrm{d}(TS) + \mathrm{d}(PV) \\ &= \mathrm{d}U - T\mathrm{d}S - S\mathrm{d}T + V\mathrm{d}P + P\mathrm{d}V \\ &= -S\mathrm{d}T + V\mathrm{d}P. \end{aligned} \tag{4}$$

The above expression can be compared to the chain rule for functions of multiple variables ($\mathrm{d}f(x,y) = \frac{\partial f}{\partial x}\mathrm{d}x + \frac{\partial f}{\partial y}\mathrm{d}y$) [15], to find the following relations

$$\left(\frac{\partial G}{\partial T}\right)_P = -S, \quad \text{and} \quad \left(\frac{\partial G}{\partial P}\right)_T = V. \tag{5}$$

This means the rate at which the Gibbs free energy of a system increases, when decreasing its temperature, is constant and given by its entropy. Furthermore, since the liquid phase of a substance generally has more entropy than its solid, a sufficient decrease in temperature will make the solid phase more stable than the liquid, allowing for a phase transition. The temperature at which this transition occurs is called the melting temperature T_M. Similarly, the rate of increase of the free energy with pressure is given by the volume of the substance.

2.2.2 Transitions of Mixtures

A mixture is a system of more than one species of material. For the sake of generality we will refer to any species A, B, etc. in this section, where the rest of the report will focus on mixtures of glycerol and water. The thermodynamic behavior of a mixture depends on the relative concentration of its constituent elements. We can describe this concentration in terms of the moles n of each species with the molar concentration x. For a mixture of two materials A and B, containing n_A and n_B moles of each, the molar concentration of substance B is given by equation 6 [13]

$$x_B = \frac{n_B}{n_A + n_B} = \frac{n_B}{n_{\text{total}}}. \tag{6}$$

The last equality of equation (6) is of general validity for any substance B in a mixture of total moles $n_{\text{total}} = \sum_i n_i$ of substance. The molar concentration ranges from $x_B = 0$ for a mixture without substance B to $x_B = 1$ of pure substance B. If the melting temperatures of substances A and B in the mixture are $T_{\text{M}}(A)$ and $T_{\text{M}}(B)$ the melting temperature of mixture $T_{\text{M}}(A+B)$ is typically lower than that of either of its constituents.
The lowering of a mixture's melting temperature depends on the molar concentrations of its constituents [13]. A liquid mixture $A + B$ dominated by A will transition to a solid-liquid combination when cooled past the melting temperature. If the crystal structure of species A is α, the solid structure of this solid-liquid combination will be $\alpha + L$, where L is the liquid structure of the mixture. Similarly, a mixture dominated by species B of crystal structure β will take on the structure $L + \beta$ when crystallizing.
The critical molar concentration x_c that separates the upper and lower boundary behavior defines the eutectic point. The melting temperature for a mixture at the eutectic point is called the eutectic temperature T_{E} and is the lowest temperature at which the mixture may exist in liquid phase. A sketch of a phase diagram for the hypothetical mixture $A+B$ is pictured in figure 2. Here the eutectic point is (x_c, T_{E}).

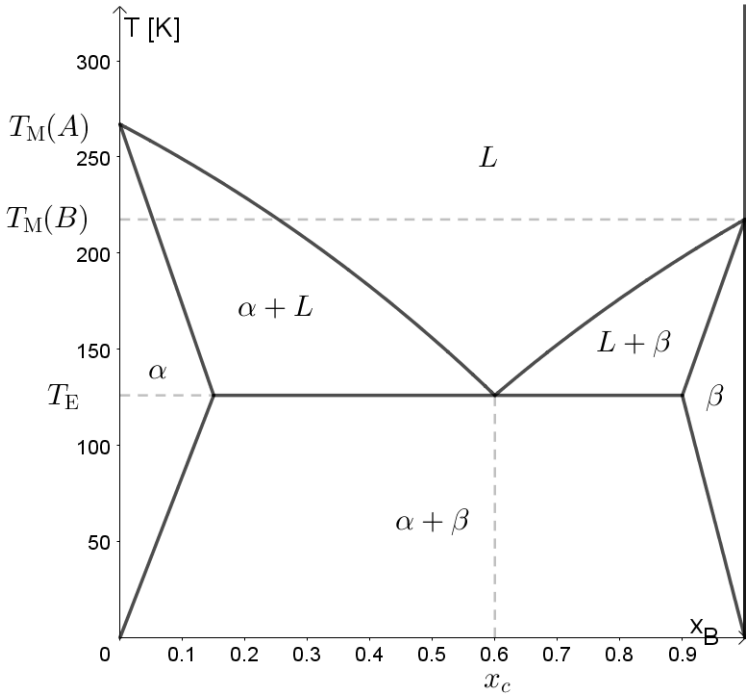

Figure 2: Sketch of solid-liquid phase diagram (plotting temperature temperature T as a function of molar concentration x_B) for hypothetical mixture $A + B$ with eutectic molar concentration x_c. Species A and B have crystal structures α and β respectively and common liquid structure L. Figure draws from Schroeder (1999) [13].

The curves separating the region of liquid phase L from the regions of solid-liquid phases $\alpha + L$ and $L + \beta$ define the melting temperature for a given molar concentration x_B. As seen in figure 2, any

cooling beyond T_E completely crystallizes the mixture. The structure that the mixture obtains upon crystallization is again determined by the composition; mixtures dominated by one species, say A, take on the crystal structure of that species, in this case α. Intermediate compositions crystallize into some combination of constituent crystal structures $\alpha + \beta$, the details of which will not be relevant for our work.

2.2.3 Glass

The phase transitions considered so far have been implicitly assumed to happen quasistatically, that is, at a slow heating rate. Quasistatic heat contributions during a substance phase transition contribute entirely towards reorganizing the molecular structure, thus not altering its temperature during the process [13]. If the temperature of a liquid substance is brought below its melting temperature but does not crystallize, we call it a supercooled liquid [3].
Continuous supercooling of a liquid increases the viscosity, a quantity analogous to internal friction of the liquid [14]. This in turn drastically increases the relaxation time τ of the substance, i.e. the characteristic timeframe in which a restructuring of the liquid to a solid state may take place. For arbitrarily large relaxation times, the microscopic liquid structure is essentially frozen in place, never quite reaching thermal equilibrium. If a supercooled liquid is frozen to such a degree that it reaches a mechanical equilibrium, we call it a glass [3]. The temperature at which a supercooled liquid transitions into a glass, and vice versa, is called the glass transition temperature T_g. This temperature is not exactly defined, as the continuous increase in viscosity happens over a range of temperatures; this range, dubbed the transformation range, is what T_g typically refers to in literature [3].
For the purposes of this project, this is enough about glass for now.

2.3 Anti-Freeze Proteins (AFPs)

Antifreeze proteins (AFPs) exist within a group of diverse proteins that have evolved in various species including but not limited to fish, insects, and plants. It has been proposed that differences between AFPs among closely related species, has come about as a result of convergent evolutionary traits. This has given rise to great variation in size and efficacy of different AFPs at a given concentration [5]. It is generally recognized that the separation of freezing and melting temperatures, induced by the anti-freeze protein is increased with size of the protein. This separation of freezing and melting temperatures is referred to as the hysteresis gap [5]. The defining feature of all AFPs is their ability to bind to ice crystals and inhibit their growth [5]. Different AFPs display different properties depending on the varying mechanisms of preventing intracellular ice formation, as well as the temperatures different species are exposed to in their environments.
Its has been postulated by Raymond and DeVries [16] that antifreeze proteins inhibit freezing by limiting the growth of ice crystals that begin to form. AFPs bind to the surface of an ice crystal by the binding surface seen in figure 3 and limit their growth. This limiting in the growth of ice crystals occurs due to an equilibrium of vapor pressure between the ice surface and the supercooled water surrounding it [16]. This vapor pressure equilibrium refers to the state at which water molecules leave the crystals surface at the same rate as they are being added [17]. Since processes like this occur at temperatures that rarely exceed -1° Celsius, we shouldn't initially expect it to have much effect at subfreezing temperatures.
Our experiments will focus on two different AFPs as well as bovine serum albumin (BSA) which is a simple bovine protein. We use BSA due to it being a similarly-sized protein with no anti-freezing effects [18]. The antifreeze proteins we are testing are arthropod (or insect) AFPs (IAFP) and type III AFPs from a suborder of a teleost fish originating in polar waters. In order to prevent any possible reactions from occurring while mixing the proteins, we will utilize phosphate-buffered saline (PBS) to stabilize the pH of our samples pH ≈ 7.4. Figure 3 below shows what a typical type III protein looks like.

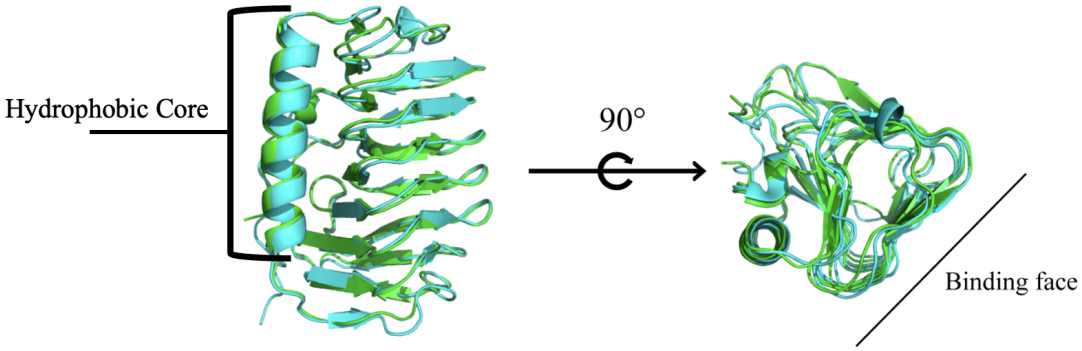

Figure 3: Stereo view depiction of a typical type III antifreeze protein, held together by a hydrophobic core [19].

3 Methodology

The following section will explain the thermalization calorimetry technique (abbr. TC) that we will employ to study how samples will be affected by the addition of proteins and buffer. It will introduce a $(T, \frac{\mathrm{d}T}{\mathrm{d}t})$-trace, or thermogram, and discuss how we will read these diagrams to make sense of the information we gather from our experiments. We will derive a mathematical expression for the physical principles behind the data that we gather. The model is built on the definition of heat capacity provided in section 2.2, and defines the relationship between temperature rate $\frac{\mathrm{d}T}{\mathrm{d}t}$ and temperature T.

3.1 Thermalization Calorimetry

The thermalization calorimetry method (TC) we utilize [4] (nicknamed the *Red Box*) measures the temperature of a liquid sample as it is being heated or cooled. The method provides two techniques for cooling a sample, relatively quick and slow referred to as quench and slow cooling respectively. Typical ranges for the cooling rate are around 10-1000$\frac{\mathrm{K}}{\mathrm{min}}$. Quench and slow cooling will be further explained in section 4.1. The experimental setup, also presented in section 4.1, produces a relatively constant heating rate due to its insulated nature and the procedures also highlighted in section 4.1. The signals being monitored are sensitive to endo- and exothermic processes which allow us to locate the temperatures at which various phase changes occur [4].
Once the data reaches the PC it is converted into temperature and numerically differentiated within a MATLAB software package. After some data processing we are left with temperature and its rate of change $(T, \frac{\mathrm{d}T}{\mathrm{d}t})$. This information is depicted on a scatterplot to reveal how the temperature is changing as it is changing.
Plotting $(T, \frac{\mathrm{d}T}{\mathrm{d}t})$ allows us to graphically visualize changes in heat capacity (often called a $(\frac{\mathrm{d}T}{\mathrm{d}t})$-trace or a thermogram [4, 10]). This gives us insight into the melting and glass transition temperatures (T_M and T_g, respectively) of the samples under investigation [4]. Figure 4 shows a rough representation of how the changes in heat capacity are understood in a thermogram plot.

3.1.1 Understanding a Thermogram

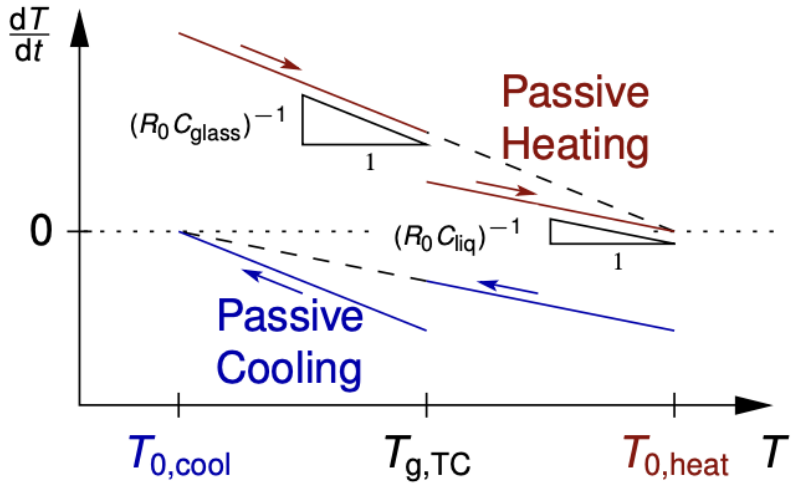

Figure 4: A graphical representation of how differences in a samples heat capacity can be observed as a change in the slope of the $(T, \frac{\mathrm{d}T}{\mathrm{d}t})$-curve. This is shown for two methods (heating and cooling) where there is a constant heat capacity in the glass (C_glass) and liquid (C_liquid) phases. At the glass transition temperature (T_g) there is a shift in the slope of the curve due to the sudden change in heat capacity between the glass phase and the surrounding supercooled liquid [4].

Figure 4 gives a rough idea of expected behavior around the glass transition that can be applied to understanding the thermograms produced by the Red Box. This is clarified in figure 5, which shows an experimentally obtained thermogram which showcases some general behavior of these types of

plots.

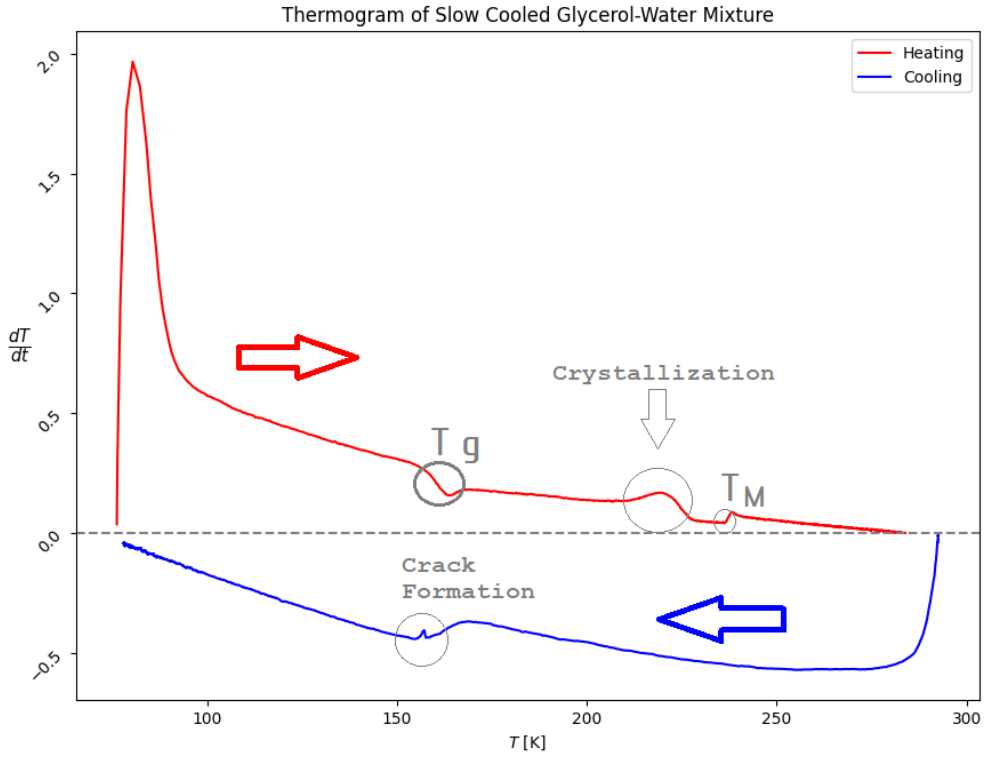

Figure 5: A thermogram of a slow cooled sample produced by the *Red Box*. Shown as T_{g} and T_{M} is the glass transition and melting temperatures respectively. The blue segment of the graph is the cooling of the sample while the red segment is the heating of the sample. Large peak in the sub 100 K range is due to transfer of the sample.

Certain points like the crack formation, crystallization, and the large peak in the lower $T < 100$ K range, are not thoroughly discussed in this report. The large peak is due to the transfer of the sample from liquid nitrogen to an insulated environment and referred to as a transfer overshoot. Crystallization can occur in the heating curve during both slow cooling and quench cooling techniques and is seen as a peak between T_{g} & T_{M}. The crack formation is only seen in slow cooling produced thermograms.

3.1.2 How Heat Capacity is Interpreted by a Thermogram

The definition of heat capacity C reveals that there is an inverse relationship between it and the change in temperature ΔT after a given heat contribution Q [4] – that is to say that they are inversely proportional $C \propto \frac{1}{\Delta T}$.

$$C = \frac{Q}{\Delta T}$$

$$\implies \quad \Delta T = \frac{1}{C} Q \tag{7}$$

To determine the amount of heat flowing into the system (Q), we use the heat rate (power) of the system $P(t) = \frac{\mathrm{d}Q}{\mathrm{d}t}$ to give us the amount of energy introduced to the system in a given amount of time. Taking the derivative of the temperature with respect to time gives us the following differential equation:

$$\Delta T = \frac{1}{C} Q \Rightarrow \frac{\mathrm{d}T(t)}{\mathrm{d}t} = \frac{1}{C}\frac{\mathrm{d}Q}{\mathrm{d}t} = \frac{1}{C} P(t) \tag{8}$$

We can then make the assumption that the amount of heat that enters the system is proportional to the difference between the equilibrium target temperature (T_0), i.e. room temperature, and its temperature at time t: $(T(t) - T_0)$.

$$P(t) = -\frac{1}{R_0}(T(t) - T_0) \tag{9}$$

The final value obtained this way is multiplied by -1 to in order to account for the fact that the difference between $T(t)$ and T_0 will result in a negative valued difference (we want it to be positive) and R_0 is the thermal resistance involved in the experiment. Combining equations 7 and 8 will give us the following relation:

$$\frac{\mathrm{d}T(t)}{\mathrm{d}t} = -\frac{1}{R_0 C}\left(T(t) - T_0\right) \tag{10}$$

With a constant heat capacity, the slope of the line at a point $(T, \frac{\mathrm{d}T}{\mathrm{d}t})$ is $-\frac{1}{R_0 C}$. Due to the characteristic changes in heat capacity during phase changes, we can readily see the change in the graph's slope to pinpoint the temperatures of interest to us (eg. T_g and T_M). Heat capacities are related to the degrees of freedom, thus with our model a change in the slope represents a phase change. For the purposes of the analysis of our various samples, we take the local minimum of the temperature-dependent derivate of the $(T, \frac{\mathrm{d}T}{\mathrm{d}t})$-trace to be defined as the glass transition temperature (see figure 5).

4 Experiment

In this section we will present the used experimental application of the methods above. Primarily, the experimental setup and procedure for thermalization calorimetry experiments. This section will also present an overview of the preparation of samples and corresponding experiments.

4.1 Setup & Procedure

Figure 6 shows the Calorimetry setup we are using in conjunction with the MATLAB software to determine our T_g and T_m temperatures. What we refer to as *The Red Box* (figure 6a), connects our thermocouple to the computer in the proper in a way that allows it to read and interpret the incoming signal. MATLAB software then calculates and records the data we represent in our $(T, \frac{dT}{dt})$-traces described in section 3.1.

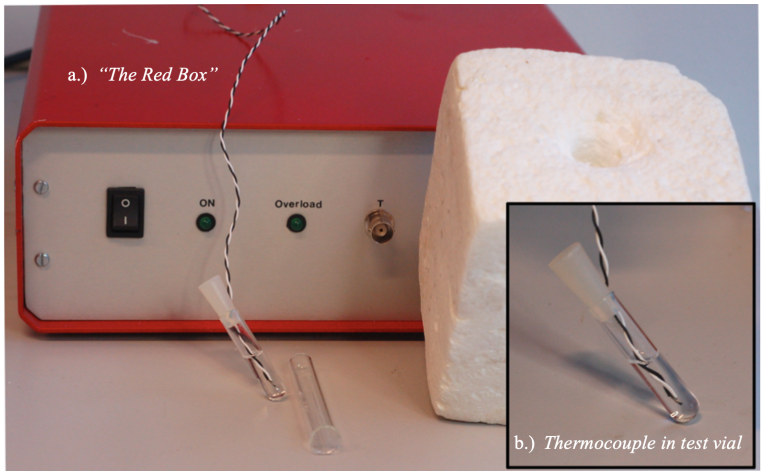

Figure 6: **a.)** *The Red Box* device consisting of an LTC2983 chip with multiple inputs to accurately measure temperature and translate the analog signal to a digital signal through an ADC (analog-digital-converter) that sends the signal to a PC through a USB cable.
b.) We utilize a "J" type thermocouple because it is sensitive to temperatures ranging from room temp (≈300 K) down to sub-freezing liquid nitrogen temperatures (in the range of $\approx 75K$)

.

4.1.1 Procedure for Thermalization Calorimetry Experiments

Based on our preliminary experiments, we designed a thorough procedure for our future Calorimetry experiments. This was done to ensure maximum possible precision.
For both slow and quench cooling methods the pre-experimental procedure is the same:

1. Disconnect thermocouple w/ plug from measurment device.
2. Clean thermocouple+plug with ethanol cleaner.
3. Dry thermocouple end with gaseous nitrogen sprayer.
4. Remove sample plug and insert clean thermocouple.
5. Ensure thermocouple is not in contact with container sides.
6. Reconnect thermocouple to measuring device, turn on device and software.
7. Fill liquid nitrogen basin if needed.

In experiments requiring more information in the cooling curve, the slow cooling method is preferable. In experiments that require a rapid temperature drop the quench cooling method is required. This method is the same as the slow cooling method, however the first step is skipped. Without the insulated test tube the sample will generally reach equilibrium with the liquid nitrogen in under a minute. The procedure is detailed below:

1. Insert sample into insulated test tube (skip when quench cooling).

2. Initialize measurement software and wait until data begins recording.
3. Insert approximately 4/5ths of the insulated sample into liquid nitrogen.
4. pre-cool isolated environment with liquid nitrogen.
5. Remove sample from liquid nitrogen and/or test tube and insert quickly into the isolated environment.
6. Cover isolated environment and allow sample to heat slowly

When Experiments are complete data is exported from measuring software as a .txt, .pdf, and .mat file. The lab is then reset to pre-experimental status.

4.1.2 Sample Preparation

Some samples used for experimentation were prepared by the authors of this report while some were prepared by the faculty at Roskilde University by Hans Ramløv.
Mixtures of glycerol-water were produced by calculating the target molar composition of glycerol in water in terms of mass. Both water then glycerol were added into a test vial on a scale to the calculated masses. The sample could then be extracted and transferred to a test vial for experimentation. For the preparation of these samples sterile syringes were used in the transfer of substances and all vials were cleaned with ethanol and dried with pressurized nitrogen to remove foreign particles.
Mixtures at $0.047x_{gly}$ and $0.23x_{gly}$ were provided by faculty at Roskilde University and result from 20% and 60% mass concentrations of glycerol and water respectively. These mixtures include phosphate buffer saline (PBS), PBS buffer & bovine serum albumin (0.5 mM), and PBS buffer & Insect anti-freeze Proteins (0.5 mM). These samples are sometimes referred to as treated mixtures below.
The buffer is added to mimic the ionic environment of a cell, keeping the pH constant. This protects the integrity of the proteins through electrostatic interactions between the proteins and ions which prevents the unexpected unfolding of the proteins during tests [20].
Mixtures of teleost fish type III anti-freeze proteins (FAFPs) were made with the use of the existing PBS buffer Mixture at $x_{\mathrm{gly}} = 0.23$. These proteins were acquired from A/F PROTEIN CANADA INC.! FAFPs were included at concentrations of 0.5 mM, 1.0 mM, 1.5 mM.

4.2 Overview of Experiments

The experiments we designed are intended to understand how AFP's affect material characteristics such as the glass transition temperature, T_{g}, and melting temperature, T_{M}. In order to do so, a series of thermalization calorimetry experiments were conducted. For each mentioned experiment both a quench-cooled and a slow-cooled measurements were taken.
The first series of experiments conducted were designed to understand the glass transition temperature as concentrations of glycerol in a sample. For this purpose experiments were conducted at a range of $x_{\mathrm{gly}} = [0.047; 0.6]$. Experiments on pure samples of water and glycerol were also conducted to understand the behavior at extremes.
Samples at a molar concentration of 0.047 and 0.23 were then chosen to study the effect of varying concentrations of glycerol with PBS buffer ions added. The buffer mixture is necessary to protect the proteins that we will investigate, therefore the sole effect of the buffer itself needed to be investigated. Experimentation with proteins in buffer mixtures at compositions of 0.047 & 0.23 glycerol then began, specifically with insect AFPs and bovine proteins (like-sized proteins with no reported anti-freeze properties). The bovine protein (BSA), was used as a reference to help specifically target the effects of the anti-freeze characteristics in the analysis of these experiments.
Finally, fish type III proteins were investigated in the 23% glycerol mixture with buffer. This mixture was chosen due to the effects seen from the past experiments; seen in section 5.2, the effects of proteins at this mixture seem to be higher than that for $x_{\mathrm{gly}} = 0.047$. Thus mixtures of 0.5 mM, 1.0 mM, and 1.5 mM concentrations were investigated.

5 Results

The following section will present the methods utilized to obtain glass transition and melting temperatures. It will then present results for the found glass transition and melting temperatures using said methods.

5.1 Obtaining the Results from Data

Raw datasets imported from MATLAB scripts running *The Red Box* were processed in Python 3.9 to obtain glass transition and melting temperatures. Using figure 5 as an example the following two subsections detail the methods used to obtain these values.

5.1.1 Obtaining T_g

Obtaining the glass transition temperature (T_g) is done through interpreting the slopes of the heating (T, $\frac{dT}{dt}$)-trace. This process is visualized below in figure 7.

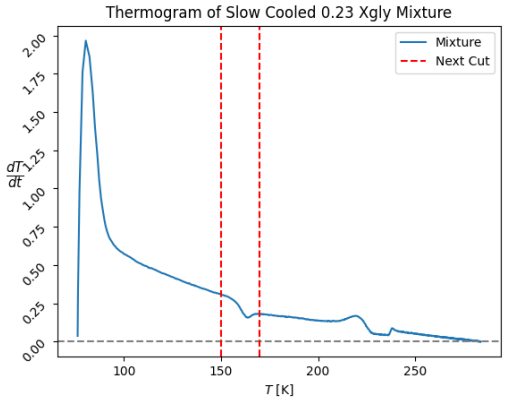

(a) Smoothed data cut to show heating of the sample, next cut depicted in red.

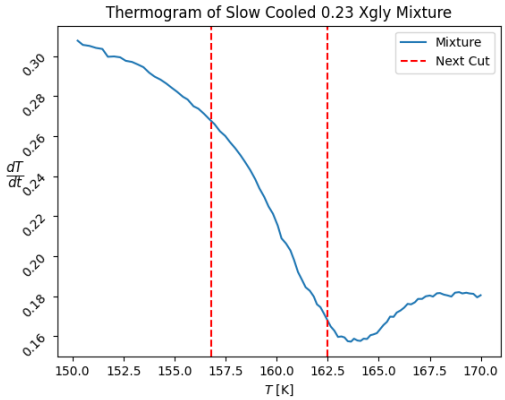

(b) Data cut around glass transition, next cut is depicted in red to precisely identify T_g.

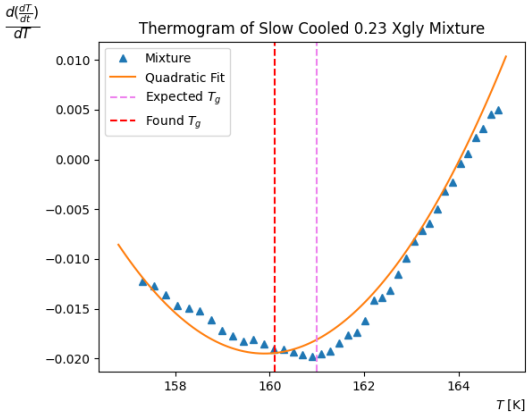

(c) Data cut with y-axis derived with respect to temperature, quadratic fit in orange while found value and expected value are in red and violet respectively.

Figure 7: Thermograms for a 0.23 mol x_{gly} mixture depicting the identification of a glass-transition temperature by isolating the glass transition and finding the point of inflection through derivation of the data.

In order to reduce noise for easier interpretation the (T, $\frac{dT}{dt}$)-trace was smoothed. This was done by using a rolling average algorithm on the data sets averaging every 20 points to one. Seen in figure 7a the smoothed (T, $\frac{dT}{dt}$)-trace shows a change in slope after 150 degrees kelvin. By cutting the data around the glass transition, the area of this change is easily visible. As discussed in section 3.1.2, the

point of most change is taken for the glass transition, therefore, the data around this point can again be cut as seen in figure 7b. To identify a consistent point for all data sets we differentiate the y-axis to $\frac{\mathrm{d}(\frac{\mathrm{d}T}{\mathrm{d}t})}{\mathrm{d}T}$. Fitting a quadratic function to this new trace allows us to pull a peak value and thereby identify the glass transition, seen in figure 7c. The deviation from the expected point seen visually and the found point stayed within a range of ± 1 K for all T_g found in experiments. Therefore we impose a uncertainty of ± 1 K for all of our measurements, seen as error bars in relevant figures below.

5.1.2 Obtaining T_M

Like the glass transition, the melting temperature (T_M) is also found by interpretation of the heating $\frac{\mathrm{d}T}{\mathrm{d}t}$-trace. However, unlike the glass transition, the melting temperature is not as vague of a point. Shown in figure 8 is the process of obtaining the melting temperature.

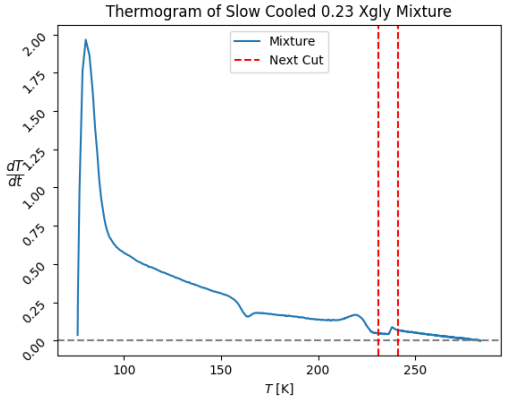

(a) Smoothed Data cut to show heating of the sample, next cut depicted in red.

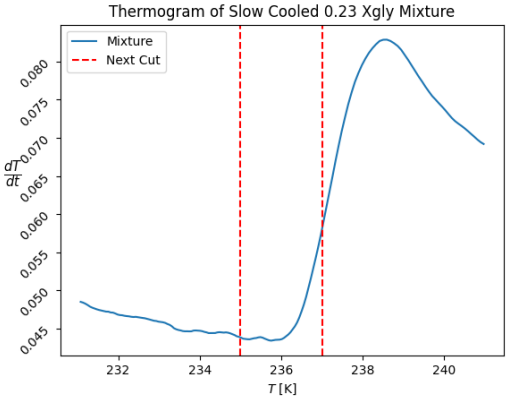

(b) Data cut around glass transition, next cut is depicted in red to precisely identify T_m.

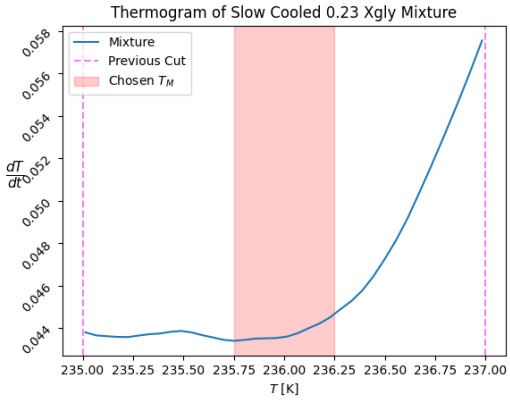

(c) Previous cut in violet, T_M found at 236K with certainty of .25K(in red).

Figure 8: Thermograms for a 0.23 mol Xgly mixture depicting the identification of a melting temperature by isolating the melting temperature and visually choosing T_M to a certainty of $\pm 0.25K$

Finding T_M begins with the heating $(T, \frac{\mathrm{d}T}{\mathrm{d}t})$-trace, smoothed by a rolling average of every 20 points to one. As discussed in section 3.1.2 the melting temperature can be seen to be the point where the rate change of temperature is close to or equal to zero and the mixture has not yet reached equilibrium with the surrounding heat source (i.e. the laboratory). The range where this occurs is identified by the "next cut" range in Figure 8a. To precisely identify a T_M for our experiments we then cut around the point again and identify it in a range of $\pm 0.25K$ uncertainty, seen as error bars in relevant figures below. This process is what is shown in figures 8b and8c.

5.1.3 Untreated Mixtures

By identifying and obtaining T_g and T_M as described above for all of our experiments, where possible, these values were able to be plotted for visual analysis in the form of a phase diagram, shown below in figure 9.

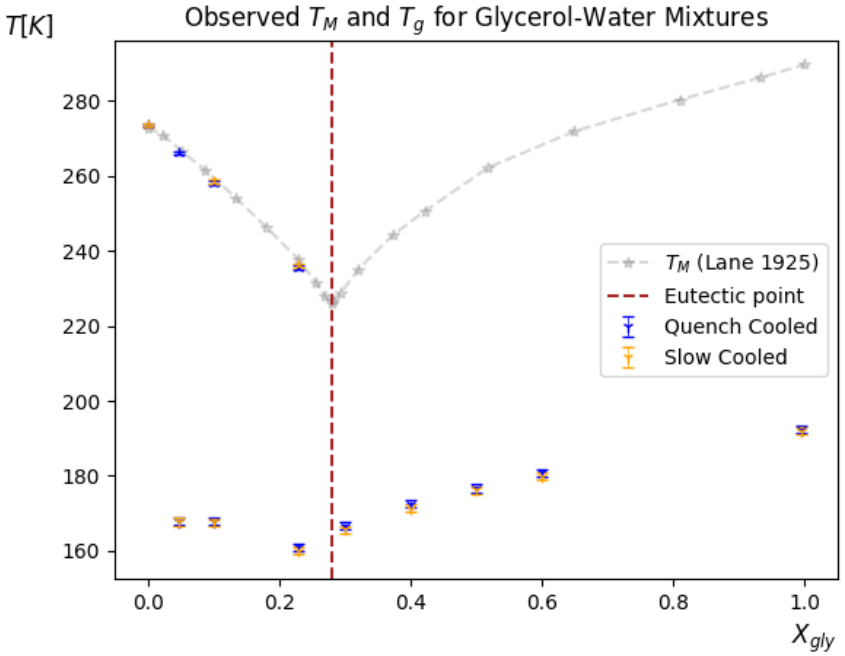

Figure 9: Resulting glass transition and melting temperatures of glycerol water mixtures as recorded by thermalization calorimetry experiments in this work.

Glass transition of $[x_{gly}]$		
x_{gly}	T_g Quench	T_g Slow
0.047	167.78	167.74
0.1	167.78	167.66
0.23	161.01	160.01
0.3	166.64	165.71
0.4	172.54	176.17
0.5	176.65	179.84
0.6	180.77	179.84
0.995	192.39	191.93

Melting (T_M) Temperatures		
x_{gly}	T_M Quench	T_M Slow
0.047	266.21	N/A
0.1	258.10	258.50
0.23	235.54	236.00

Table 1: Glass transition and melting temperatures (T_g) and (T_M) of different glycerol concentrations. The table to the right shows the melting temperatures of (x_{gly}) concentrations of glycerol and water below the eutectic point.

5.2 Treated Mixtures

The following data results from mixtures treated with our buffer, buffer & BSA proteins, and buffer & insect AFPs. This can be seen in figure 10. The data resulting from the teleost fish type III AFP concentrations will be presented seperately in section 5.3.

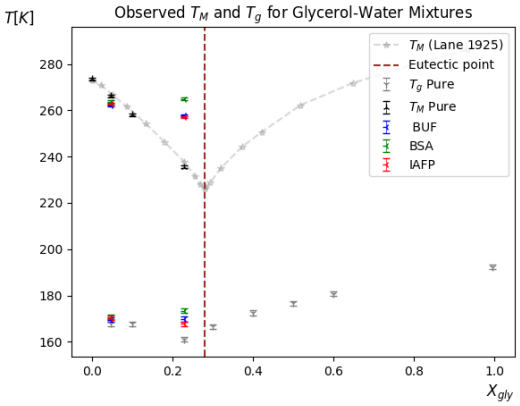

(a) T_g and T_M for Glycerol-Water Concentraions treated with proteins and/or Buffer ions

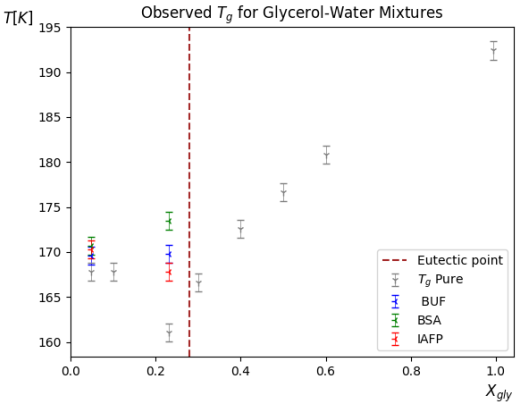

(b) T_g for Glycerol-Water Concentraions treated with proteins and/or Buffer ions

Figure 10: Observed glass transition and melting temperatures for both treated and untreated mixtures (for reference). Mixtures with only buffer are depicted in blue. Buffer mixtures with BSA and Insect AFPs are depicted in green and red respectively.

5.2.1 Melting Temperatures

Untreated mixtures tend to have a lower melting temperature as they reach a concentration closer to the eutectic point, seen in figure 9. Treated mixtures, however, do not follow this same trend, seen below in figure 11. The increase of glycerol in the mixture may also have some impact on the effect of proteins.

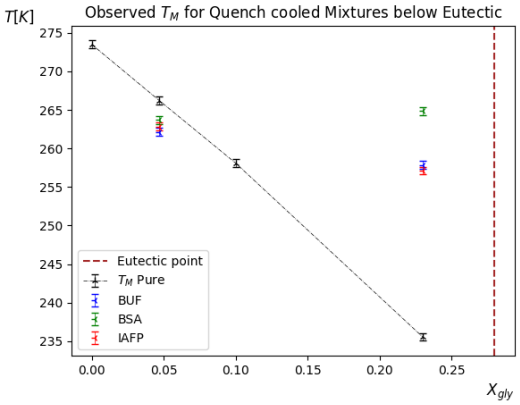

(a) T_M for Quench cooled Mixtures and Treated Mixtures by, concentration glycerol.

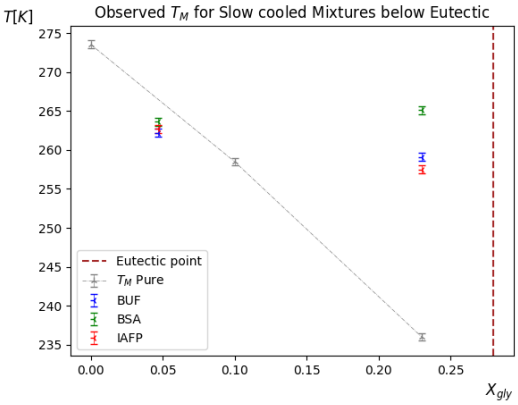

(b) T_M for Slow cooled Mixtures and Treated Mixtures, by concentration glycerol.

Figure 11: Observed melting temperatures for both treated and untreated mixtures (for reference). Mixtures with only buffer are depicted in blue. Buffer mixtures with BSA and Insect AFPs are depicted in green and red respectively.

Quench-cooling				
Melting temperatures of samples (K)				
x_{gly}	Untreated	**Buffer**	**BSA**	**IAFP**
0.047	266.21	262.13	263.69	262.85
0.23	235.54	257.85	264.85	257.10

The table above shows the Melting temperatures of the quench-cooled mixtures presented in figure 11a. Samples names are colored to match the points the figure just mentioned.

5.2.2 Glass Transition Temperatures

Treated mixtures under investigation were found to have higher glass transitions than their untreated counter parts. Visual inspection of Figure 12 reveals that again the increase of glycerol has some impact on the effect of proteins on the T_g.

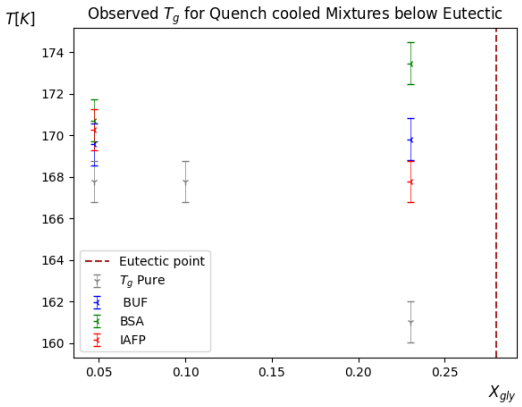

(a) T_g for Quench cooled Mixtures and Treated Mixtures by, concentration glycerol.

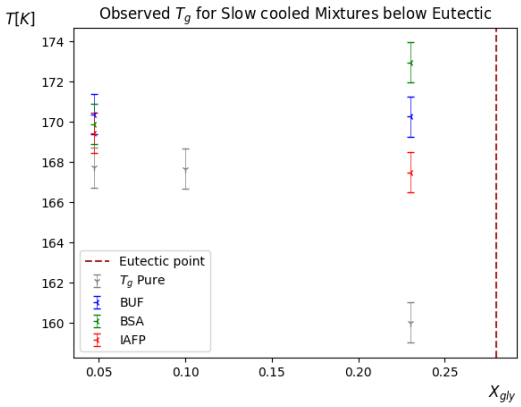

(b) T_g for Slow cooled Mixtures and Treated Mixtures, by concentration glycerol.

Figure 12: Observed Glass Transition temperatures for treated and untreated mixtures (for reference). Buffer Mixtures are depicted in blue. Bovine Protein Mixtures with buffer are depicted in green. Insect AFPs are depicted in red.

Quench-cooling				
Glass transition temperatures (K)				
x_{gly}	Untreated	Buffer	BSA	IAFP
0.047	167.78	169.56	170.72	170.27
0.23	161.01	169.81	173.47	167.78

5.3 Fish type III Anti-Freeze Proteins

The T_g and T_M of a $0.23 = x_{\text{gly}}$ concentration mixture with buffer changed as the concentration of fish type III AFPs was changed. From visual inspection of figure 13 we can see that both T_g and T_M decreased from their corresponding buffer T_g and T_M. However, at the 0.5 mM concentration the T_g is higher and T_M lower than that of the 1.0 mM and 1.5 mM concentrations. Following figure 13b is a table of the data presented in the figure.

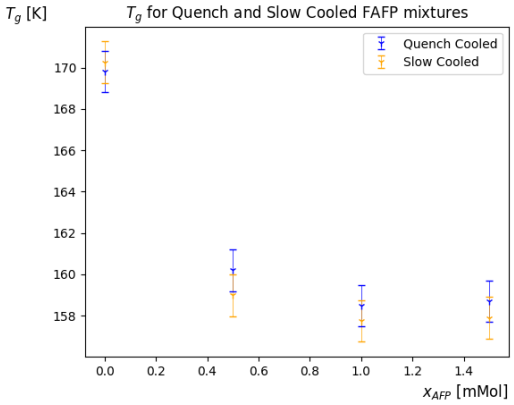

(a) T_g for Slow and Quench Cooled Fish AFPs in mixture.

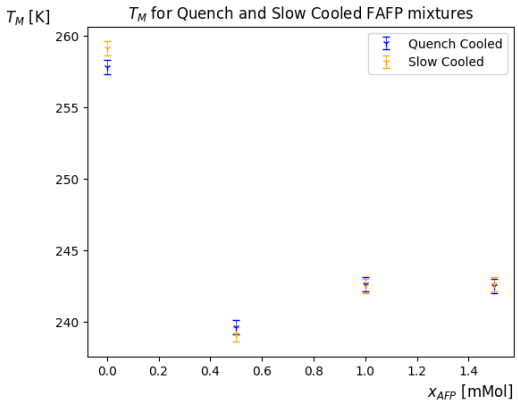

(b) T_m for Slow and Quench Cooled Fish AFPs in mixture.

Figure 13: T_g and T_M of a range of 0.5-1.5 mMol Concentrations of Fish Type III AFPs. Quench Cooled data in blue and Slow Cooled data in Orange

$FAFP\ in\ [0.23]_{gly}$				
	T_g		T_M	
x_{FAFP}	Quench-Cooled	Slow-Cooled	Quench-Cooled	Slow-Cooled
0.0	169.81	170.27	259.11	257.85
0.5	160.19	158.98	239.10	239.60
1.0	158.49	157.73	242.52	242.64
1.5	158.69	157.89	242.60	242.51

6 Analysis

This section aims to answer the problem formulation stated in section 1.1 with the data presented in section 5. We first investigate the effect of the buffer of choice, phosphate buffer saline (PBS). Next we look at how the inactive bovine serum albumin proteins (BSA) affect our mixtures with buffer. Section 6.3 compares buffer samples with 0.5 mM insect anti-freeze protein to the mixtures already discussed in sections 6.1 and 6.2. Finally, section 6.4 investigates the effect of varying concentrations of AFP, namely teleost fish type III AFPs.
The effects are evaluated by the apparent change in glass transition and melting temperatures, T_{g} and T_{M}, between samples of a certain treatment and control samples without said treatment. For example, the "effect" that BSA has on the glass transition temperature of a mixture with buffer is determined by how big the difference ΔT_{g} is between a sample with buffer and BSA, and one with buffer and no BSA.

6.1 Effect of Phosphate Buffer Saline

As explained in section 4.2, the buffer is applied to our samples to ensure a stable environment for the AFPs. We will here investigate how this buffer affects our mixture. We start with figure 14, which combines data from the phase diagrams depicted in figures 9 and 10 for the untreated mixture samples, and the mixtures with buffer solution, respectively.

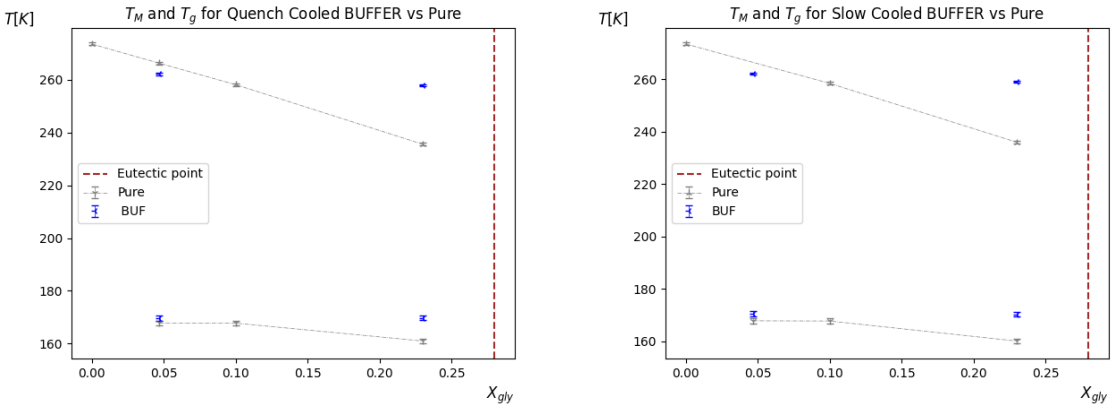

(a) Untreated mixtures versus mixtures with buffer, as achieved by quench cooling.

(b) Untreated mixtures versus mixtures with buffer, as achieved by slow cooling.

Figure 14: Phase diagrams comparing untreated glycerol-water mixtures (grey) to mixtures with buffer (blue). Melting temperatures are above 200 K and glass transition below. Quench cooled melting temperatures are depicted in gray for reference.

As we can see from both subfigures of figure 14, the buffer notably shifts the melting and glass transition temperatures of our particular mixture compositions. In all cases T_{g} is increased by the addition of buffer, as can be seen from the summarized data in table 2.

Effect of Buffer on Mixture				
	Glass transition		Melting	
x_{gly}	ΔT_{g}(quench) [K]	ΔT_{g}(slow) [K]	ΔT_{M}(quench) [K]	ΔT_{M}(slow) [K]
0.047	1.78	2.64	-4.08	N/A
0.23	8.80	10.26	22.31	23.11

Table 2: Changes in glass transition and melting temperatures, ΔT_{g} and ΔT_{M}, for varying molar compositions x_{gly} when buffer solute is added to the mixture. Values obtained through quench and slow cooling methods are displayed separately.

We have insufficient data for a meaningful statistical analysis. Nevertheless, the data we have suggests that the buffer increases the value of the glass transition temperature. Furthermore, the amount

by which the buffer exhibits this effect, seems to be pronounced by the increase of glycerol in the mixture, as well as the cooling rate. For compositions of 4.7% glycerol, T_g was raised by 2.21 K, while compositions of 23% were raised by 9.53 K, when averaging over cooling rates. When averaging over compositions, addition of buffer increases T_g by 5.29 K in quench cooled samples, and by 6.45 K in slowly cooled samples. This suggests that the buffer increases T_g slightly more in slowly cooled samples compared to quench cooled ones.
The effect of the buffer on the melting temperature T_M is not as clear. The data suggests that the buffer increases the melting temperature of 23% glycerol mixtures by 22.71 K when averaging over slow and quench cooling methods. Unfortunately, the data for ΔT_M(slow) when buffer is added to the 4.7% mixture is not available; this is because of an error that occurred during the slow cooling calorimetry experiment for this mixture. The program shut off before the mixture could fully melt, thus T_M is not available for the given sample, but T_g is. Nonetheless, we see that the presence of the buffer in the quench cooled 4.7% glycerol mixture lowers the melting temperature by 4.08 K. The precise effect of the buffer on the melting temperature of water-rich glycerol-water mixtures is thus disputed; it appears to increase T_M for compositions approaching the eutectic $x_{gly} \to x_c$, and decrease it for compositions dominated by water $x_{gly} \to 0$.
To summarize, our data suggests that the addition of phosphate buffer saline to water-rich compositions of glycerol-water mixtures has the following effects on their solid-liquid phase transition temperatures. Firstly, the glass transition temperature T_g is increased by the presence of the buffer, the degree of which appears to be enhanced with glycerol content. Secondly, the melting temperature T_M appears to change, increasing with high glycerol content, but decreasing slightly with low glycerol content. Additionally, these effects appear to be pronounced in slowly cooled samples, when compared to quench cooled samples.

6.2 Effect of Constant Concentration Bovine Serum Albumin Solute

Anti-freeze proteins are typically much larger than glycerol or water molecules (see section 2.3). While the mechanism that allows for anti-freeze properties is expected to affect temperature behavior, it is the purpose of this section to determine the effect of a protein without such properties on our mixture. Thus we will compare data provided from our mixtures with buffer solution, to those with buffer solution and BSA. Figure 15 shows a mixture phase diagram with the data points for the mentioned samples.

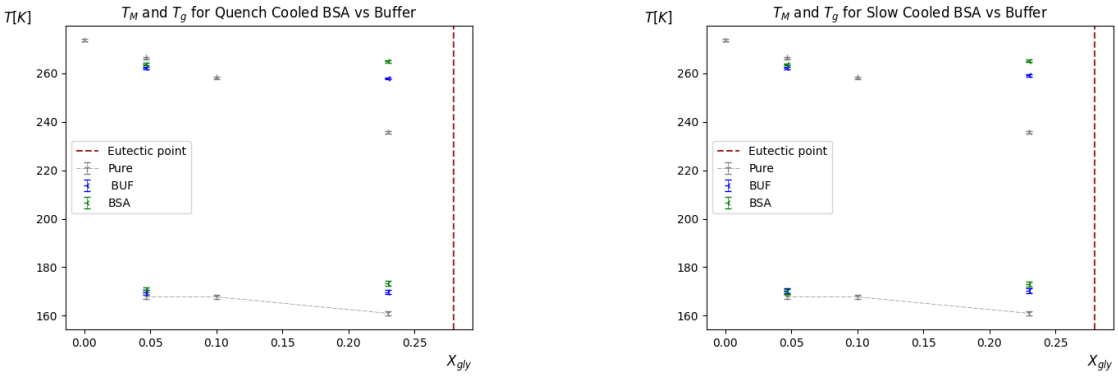

(a) Mixtures with buffer versus mixtures with buffer and BSA, as achieved by quench cooling.

(b) Mixtures with buffer versus mixtures with buffer and BSA, as achieved by slow cooling.

Figure 15: Phase diagrams comparing glycerol-water mixtures with buffer (blue) to mixtures with buffer and 0.5 mM BSA solute (green). Quench cooled melting and glass transition temperatures are depicted in gray for reference.

As before we present the changes in phase transition temperatures ΔT_g and ΔT_M in table 3. For example, the glass transition temperature in the quench cooled 4.7% glycerol mixture with buffer is increased by 170.72 K − 169.56 K = 1.16 K when adding 0.5 mM BSA solute.

Effect of BSA on Buffer Mixture				
	Glass transition		Melting	
x_{gly}	ΔT_{g}(quench) [K]	ΔT_{g}(slow) [K]	ΔT_{M}(quench) [K]	ΔT_{M}(slow) [K]
0.047	1.16	-0.50	1.56	1.42
0.23	3.66	2.68	7.00	5.99

Table 3: Changes in glass transition and melting temperatures, ΔT_{g} and ΔT_{M}, for varying molar compositions x_{gly} when 0.5 mM BSA is added to the mixture with buffer. Values obtained through quench and slow cooling methods are displayed separately.

As can be seen from the table, the presence of BSA typically raised the transition temperatures of our samples. The average change in T_{g} across the given compositions and cooling rates is 1.75 K. In one sample, namely the slowly cooled 4.7% glycerol mixture, the difference in T_{g} between the buffer sample and the buffer sample with BSA was 169.88 K − 170.38 K = −0.50 K.
The addition of BSA appears to affect the melting temperature, with an average increase in T_{M} of 2.00 K when compared to the control buffer mixtures. In particular, this effect appears to increase with glycerol content; increasing by 1.49 K for 4.7% glycerol mixtures and 6.50 K for 23% mixtures, both when averaging over given cooling rates.
Overall we find weak trends in our data suggesting that the transition temperatures T_{g} and T_{M} are raised when adding 0.5 mM BSA to our water-rich glycerol-water mixtures prepared with buffer.

6.3 Effect of Constant Concentration Insect-AFP Solute

In the previous section we investigated the effect of adding a protein solute of constant concentration which does not exhibit anti-freeze properties. We will now investigate the effect of 0.5 mM insect AFP (IAFP) solute in our buffer mixture. We provide comments on the comparison of the buffer mixture with IAFP to both the buffer mixture (see section 6.1) and the buffer mixture with BSA (section 6.2). Figure 16 shows a mixture phase diagram with values of T_{g} and T_{M} obtained through quench and slow cooled calorimetry experiments on insect AFP samples.

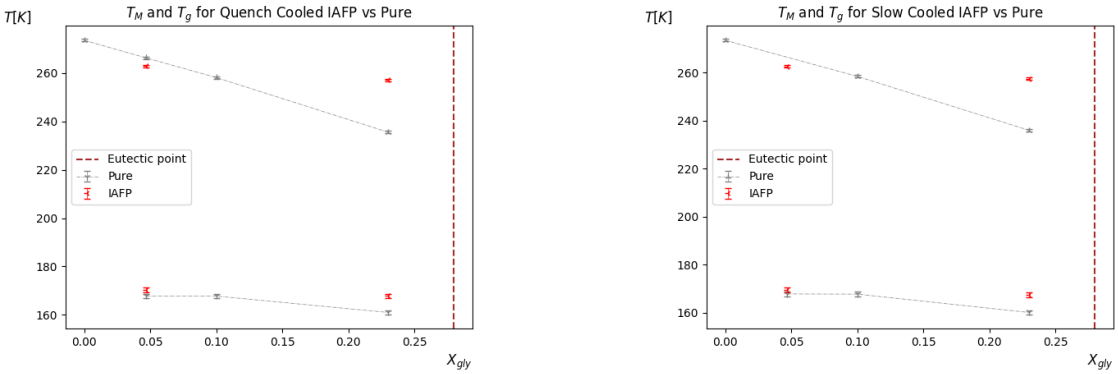

(a) Mixtures with buffer versus mixtures with buffer and BSA, as achieved by quench cooling.

(b) Mixtures with buffer versus mixtures with buffer and BSA, as achieved by slow cooling.

Figure 16: Phase diagrams depicting glycerol-water mixtures with buffer and 0.5 mM insect AFP (IAFP) solute (red). Melting and glass transition temperatures are distinguished by their temperature values, for reference we have $T_{\text{g}} < 200\text{ K} < T_{\text{M}}$. Melting and glass transition temperatures of untreated mixtures are depicted in gray for visual aid.

As we can see in all cases, the mixtures with buffer and insect AFPs have different melting and glass transition temperatures compared to their untreated counterparts. We have noted that the presence of the buffer typically increases T_{g} in our mixtures, an effect which seems to increase with decreased cooling rate and increased glycerol content. The effect of buffer addition on T_{M} is undetermined, though it appears to decrease with low glycerol content and increase with high content. We summarize the changes in relevant temperatures between mixtures with buffer and mixtures with buffer and IAFP in table 4.

Effect of 0.5 mM Insect AFP on Buffer Mixture				
	Glass transition		Melting	
x_{gly}	ΔT_{g}(quench) [K]	ΔT_{g}(slow) [K]	ΔT_{M}(quench) [K]	ΔT_{M}(slow) [K]
0.047	0.71	-0.94	0.72	0.50
0.23	-2.03	-2.79	-0.75	-1.61

Table 4: Changes in glass transition and melting temperatures, ΔT_{g} and ΔT_{M}, for varying molar compositions x_{gly} when 0.5 mM insect AFP is added to the mixture with buffer. Values obtained through quench and slow cooling methods are displayed separately.

The only difference in the treatment processes of the compared samples in table 4 is the addition of insect anti-freeze proteins of 0.5 mM concentration. Thus the changes in transition temperatures reflect the effect of anti-freeze *proteins*, as opposed to the anti-freeze effect that the proteins possess. We now investigate the former of the two.
The addition of insect AFPs appears to decrease T_{g}, with an average change of -1.26 K. This effect appears to be less pronounced in quench cooled samples, in fact showing an increase in 4.7% glycerol with IAFP treatment.
Assuming that the IAFP solute does decrease T_{g} in our mixtures, we note that this effect appears to increase in magnitude with glycerol content. T_{g} is decreased by 0.12 K in 4.7% glycerol mixtures with buffer, and by 2.41 K in 23%.
The effect on the melting temperature is unclear. The average change in T_{M} across available samples is -1.14 K. The data is however unevenly distributed among glycerol compositions, suggesting an increase for low glycerol content, and a decrease for near eutectic mixtures.
We now turn to a comparison of the buffer mixtures with BSA to those with insect AFP, both of 0.5 mM. The changes in transition temperatures are displayed in table 5.

"Antifreeze Property" Effect on 0.5 mM BSA Buffer Mixture				
	Glass transition		Melting	
x_{gly}	ΔT_{g}(quench) [K]	ΔT_{g}(slow) [K]	ΔT_{M}(quench) [K]	ΔT_{M}(slow) [K]
0.047	-0.45	-0.44	-0.84	-0.92
0.23	-5.69	-5.47	-7.75	-7.60

Table 5: Differences in glass transition and melting temperatures, ΔT_{g} and ΔT_{M}, between buffer mixtures with BSA and Insect-AFPs, at varying molar compositions x_{gly}. Values obtained through quench and slow cooling methods are displayed separately.

Both the sample treatments of comparison in table 5 contain 0.5 mM protein solute. Bovine serum albumin and insect anti-freeze proteins are of similar size. The main difference between them is the "anti-freeze property" of AFPs. Thus to some extent, the differences reported in table 5 represent the effect that this anti-freeze mechanism itself has on the temperatures of interest. We will discuss the validity of this comparison later.
Within this comparison, every sample with IAFP was found to have lower glass transition and melting temperatures than their corresponding mixture with BSA. This suggests that the anti-freeze property itself decreases both T_{g} and T_{M}, an effect that increases in magnitude with glycerol content. This is observed when comparing the magnitudes of the average changes for varying compositions. On average T_{g} and T_{M} is decreased by 0.45 and 0.88 kelvin, respectively, in 4.7% glycerol mixtures, but by 5.58 and 7.68 kelvin in 23% glycerol. We stress that this should not be taken as definitive evidence that the anti-freeze property is the *cause* of these effects. The comparison of BSA to insect AFPs is entirely speculative, based solely on a rough estimate of the spacial geometry of the proteins. Our data does however suggest that there is some difference in how these two proteins affect the transition temperatures of interest. We will discuss this point further in the report.

6.4 Effect of Fish-AFPs at Constant Molar Composition

In the previous section we investigated the effect that the anti-freeze mechanism of an AFP has on varying water-rich compositions of glycerol-water mixtures, when the protein concentration in the mixture is a constant 0.5 mM. In this section we will aim to specify to what extent the concentration

of AFPs, denoted [FAFP], affect the transition temperatures of interest, T_g and T_M. In particular we use the type III fish AFPs described in section 2.3 with concentrations of 0.5, 1.0, and 1.5 mM. Figure 17 collects data for slow and quench cooled samples, depicting the glass transition (figure 17(a)) and melting temperatures (figure 17(b)) for buffer mixtures with fish AFP of concentration [FAFP]. Here the temperatures depicted at [FAFP] = 0 correspond to the values of T_g and T_M in the buffer mixture without any proteins, discussed in section 6.1.

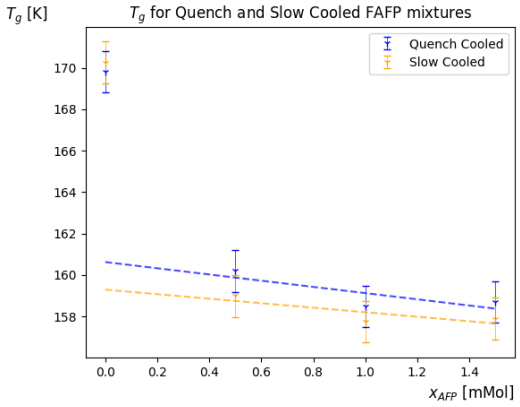

(a) Glass transition temperatures of buffer mixtures with mM fish AFP concentration [FAFP]. Quench and slow cooled samples are depicted in blue and orange, respectively. T_g at [FAFP] = 0 is given by the untreated mixtures with buffer and depicted with inverse triangles up in the upper left corner and not on the fit.

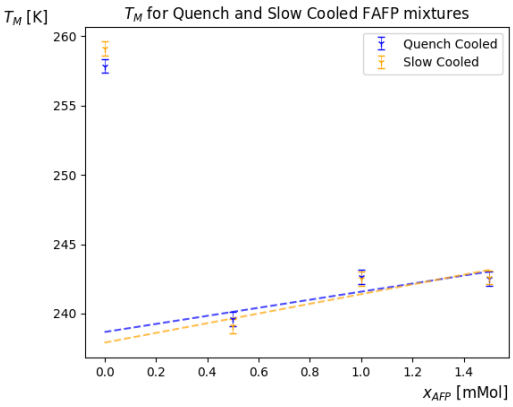

(b) Melting temperatures of buffer mixtures with fish AFP concentration [FAFP]. Quench cooled samples are depicted in blue and slow cooled with in orange. Values of T_M without FAFP are given by the untreated mixtures with buffer and depicted with inverse triangles up in the upper left corner and not on the fit.

Figure 17: Scatter plots of transition temperatures, T_g and T_M, as a function of type III fish AFP concentration [FAFP]. All quench cooled samples are depicted with red and all slow cooled ones with blue.

The data for transition temperatures of samples with non-zero fish AFP concentration in figure 17 is depicted with a least squares linear fit for each method of cooling. The fits for T_g ([FAFP]) exhibit a weak linear relationship, with coefficients of determination r^2 of 0.647 and 0.642 for the quench and slow cooled data, respectively. This is expected with a limited data set. We can thus not determine a relationship between T_g and [FAFP]. We note however that both regression fits have negative trends, $-1.50\frac{\mathrm{K}}{\mathrm{mM}}$ in the case of the quench cooled sample, and $-1.09\frac{\mathrm{K}}{\mathrm{mM}}$ for the slow cooled.
The melting temperature appears to increase slightly with increased FAFP concentration. Despite this, T_M for all samples appears to be lower than that of the untreated $x_{\mathrm{gly}} = 0.23$ glycerol-water mixture with buffer. The trend suggested for the melting temperature by the regression fit in figure 17(b) is $2.91\frac{\mathrm{K}}{\mathrm{mM}}$[FAFP] for the quench cooled samples, and $3.50\frac{\mathrm{K}}{\mathrm{mM}}$[FAFP] for the slow.

In summary, we do not find significant evidence to suggest that varying the concentration of fish anti-freeze protein alters the transition temperatures T_g and T_M in the range of [0.5;1.5] mM solute. Our values of T_g do decrease with an average rate of 1.30 K per mM fish AFP over cooling rates. Similarly, T_M shows an average increase of 3.21 K per mM solute. The reasons for these changes may be due to chance occurrence in the sampling process. We leave it for further research to better establish whether or not the concentration does indeed affect these temperatures.

7 Discussion

In the following section we will discuss the uncertainties in our data, arbitrary choices made by this report and others, and possible future research into the effect of anti-freeze proteins on the glass transition temperature.

7.1 Uncertainties

There are a number of possible uncertainties presented to us throughout our experiments. Possible contamination of the sample cell with dust or chemical impurities could have an adverse effect on the temperatures when we measure phase changes. Contaminants can act as nucleation sites for ice crystals to form. Even vibrations from the surrounding environment can cause nucleation sites to form and throw off the results. This is why it is crucial to include the cleaning procedure of the equipment as described in section 4.1.
Unfortunately we have no estimate for the inherent variability of T_{g} and T_{M}, due to tests of individual sample treatments only being conducted one time. If we had ample time to test and retest several samples we could more accurately attest to the accuracy of the data we have obtained. Also our analysis shows a small variability between the T_{g} of our time-averaged points and that of the parabola, aka quadratic function, we fit our data to (as seen in figure 7). Referring to the figure, we see different values between expected T_{g} and actual values for T_{g} found. This is a standard deviation of around ± 1 K.

7.1.1 Cooling rates

The exact cooling/heating rates during the quench and slow cooled sample treatments, measured in $\frac{\mathrm{K}}{\mathrm{min}}$, have not been discussed so far. The time span for a typical quench cooling process is in the order of a few seconds, while that of a slow cooled process is upwards of 30 minutes. Since cooling processes are driven to equilibrium by liquid nitrogen of temperature ≈ 75 K, from room temperature around 300 K, we can roughly estimate the average cooling rates as,

$$\left.\frac{\Delta T}{\Delta t}\right|_{\mathrm{quench}} \approx -1200\frac{\mathrm{K}}{\mathrm{min}}, \quad \text{and} \quad \left.\frac{\Delta T}{\Delta t}\right|_{\mathrm{slow}} \approx -10\frac{\mathrm{K}}{\mathrm{min}}.$$

The quench cooling rate is thus approximately a hundred times greater than the slow cooling rate. From our theoretical understanding of the formation of glass (section 2.2.3), we should expect glass formation to be significantly more likely in the quench cooled samples as a result. How does this affect the conclusion we can draw from our data?
The various treatment procedures of the samples investigated in this project constitute a reasonable sample size for comparing the effect of differing cooling rates. We associate, with each sample treatment, the difference d in a temperature of interest, between the quench and slow cooled processes of that sample treatment. For example, if we wish to compare the apparent difference in glass transition temperature between a quench and slow cooled sample, we write $d_{\mathrm{g}} = T_{\mathrm{g}}(\mathrm{quench}) - T_{\mathrm{g}}(\mathrm{slow})$. These differences are visualized in figure 18 for varying molar compositions of glycerol-water mixtures.

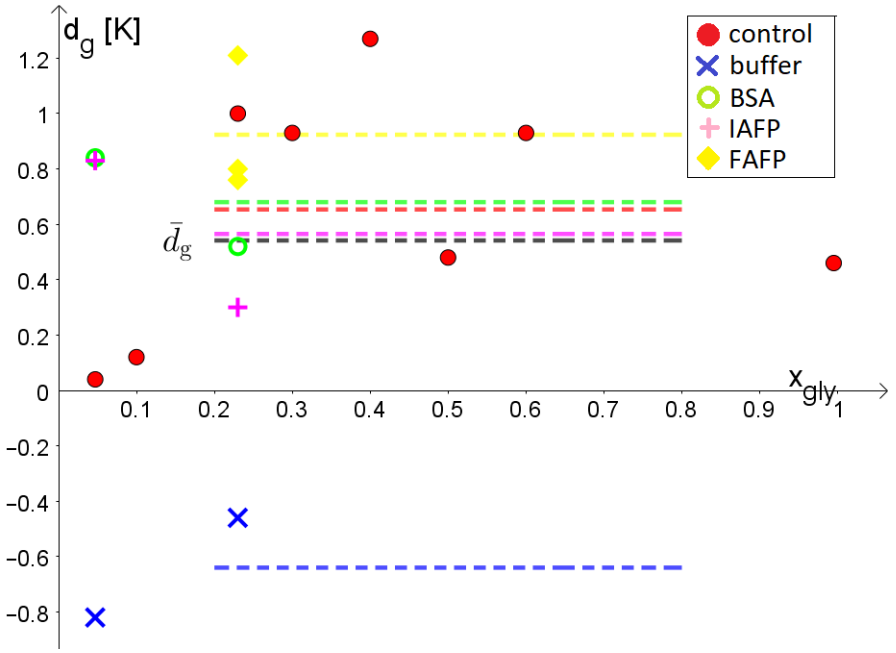

Figure 18: Difference d_g in glass transition temperature T_g between samples that have been frozen via quench and slow cooling rates. Positive values of d_g indicate greater T_g in the quench cooled sample than slow.

The mean of all differences is depicted by a broken line in black. As can be seen, T_g is greater in quench cooled samples than slow cooled samples for all treatments except for the mixtures with only the buffer, PBS, depicted in blue. The buffer treatments stand out in figure 18 because of this. The sample furthest away from the mean $(x_{gly}, d_g) = (0.047, -0.82)$, would be considered an outlier of the dataset if the distribution of d_g was independent of the molar composition of the mixture. Our sample size is not large enough to determine the dependency or lack thereof between these variables. Nevertheless we emphasize the various experiments conducted on glycerol-water mixtures of $x_{gly} = 0.23$.
According to our data T_g is higher in a quickly cooled 23% glycerol mixture than in one cooled at a slower rate. This applies when the treatment of the mixture is any one of the procedures covered in the report, except for the pure mixtures with buffer solute. This should be expected from the theoretical description of glasses covered in section 2.2.3, since a fast cooling rate will allow the viscosity to reach the critical level to be considered a glass at an earlier and higher temperature. This is in opposition to a slow cooling rate, where the viscosity increases at a rate low enough for some microscopic crystal restructuring to take place. The fact that the buffer mixtures appear to deviate from this behavior is not explained by the data and offers a possibility for further research.
In the case of the addition of fish AFP to the buffer mixture (depicted in yellow on figure 18) the difference in reported T_gs 0.92 K $\pm$ 0.2 K. This is a significant uncertainty in terms of comparing cooling rates, thus we cannot say exactly what the influence of cooling rate is on our mixtures. We note some regularity in the deviance that may prove fruitful for future research projects.

7.2 Arbitrary Choices

Certain choices when defining where transitions occur or when defining concentrations can be rather arbitrary. For example, the method of thermalization calorimetry as developed by the glass and time department at Roskilde University comes with a somewhat vague and arbitrary definition of the glass transition [4]. Seen in figure 19 the glass transition can be defined anywhere in the shown range. For the purpose of this report we chose a T_g where the slope of the $(T, \frac{\mathrm{d}\frac{\mathrm{d}T}{\mathrm{d}t}}{\mathrm{d}T})$-trace showed the largest change whereas in Jakobsen et al. (2016) [4] they chose a point at the bottom of this curve. The reason for this was to be able to use a method that chose T_g the same way for all of our samples.

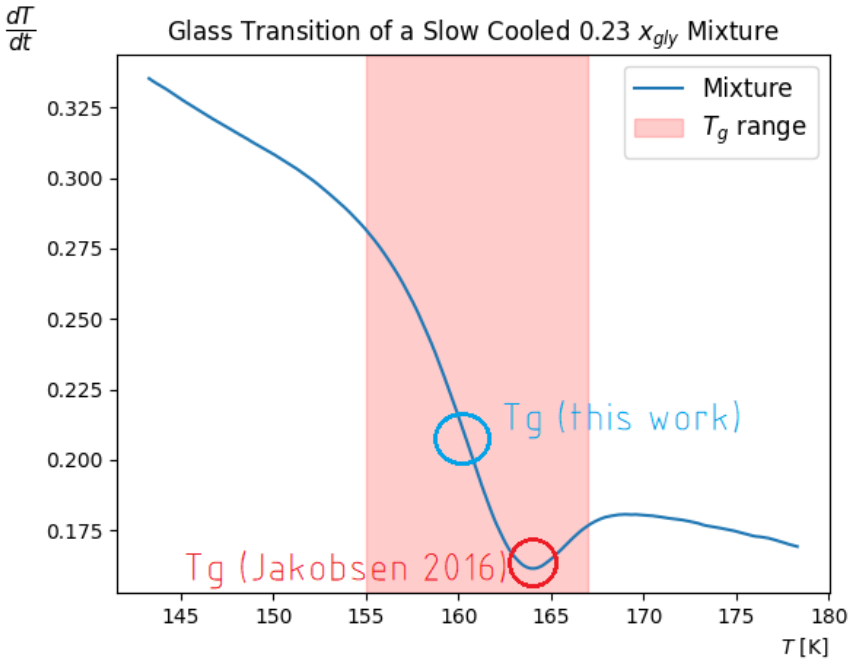

Figure 19: Glass transition of a slow cooled $0.23x_{gly}$ mixture with glass transition depicted in red as a range of where this behavior is define. Glass transition as we defined it and as [4] defines it circled and labeled.

Unlike T_g, T_M was chosen visually, using the same method as Jakobsen et al. (2016) [4]. Comparison of our data to that of others [2, 6–9] reveals that our melting temperatures are remarkably consistent while our glass transition temperatures are consistantly lower than other thermalization calorimetry experiments. This is due to the difference in our chosen T_g. Data from [2, 6–9] is plotted with our own below in figure 20.

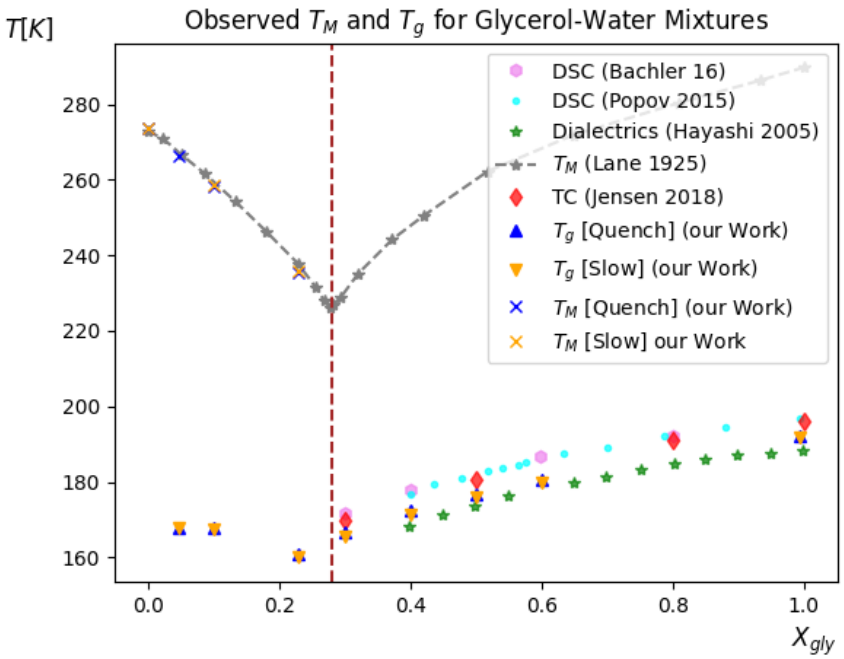

Figure 20: T_g and T_M for all recorded experiments done in this report, denoted (our work), and data from similar experiments using Differerntial Scanning Calorimetry, DSC, Dialectrics, and Thermalization Calorimetry. Figure shows that our data is consistently lower than that of other Calorimetry experiments due to difference in where measurment is taken. Other experiments in the area are [2, 6–9]

Another choice made in this report was to represent concentrations in the molar percentage, we denote x_{gly}, instead of a mass percentage. For example, our $0.047x_{gly}$ and $0.23x_{gly}$ concentrations are 20% and 60% Glycerol by mass. This is done to stay in line with precedents set by previous research.

7.3 Further Research

Research into the effects of AFPs on sub-eutectic water-glycerol concentrations is ongoing and much can be done in this field utilizing different analysis techniques and procedures. One such technique for future studies is to take dielectric spectroscopy measurements of the various samples we tested to determine how an applied electric field effects the sample at varying frequencies [21]. This could reveal a wealth of additional information on material structure, dipole-moment orientation, ion displacement and more. We were successful in taking one dielectric measurement of a 23% glycerol sample. Sadly the data we gathered from this experiment was insufficient to conclude anything useful as it relates to our TC measurements, but a minor success for us was proving the efficacy of the method. Unfortunately our experiments were discontinued due to semester time-constraints, but we hope that future research in this area could reveal relevant data on the material effects of AFPs on sub-eutectic glycerol water mixtures.

8 Conclusion

This report has established theoretical knowledge necessary to the understanding of the methods used in the investigation of glycerol-water mixtures, specifically the effect of AFPS on the glass transition and melting temperatures, commonly denoted by the symbols T_{g} and T_{M}, respectively. It has then continued and outlined methods used. An experimental structure was designed and presented. The results of the experiment were processed and presented.
Through treatment of data extracted from thermalization calorimetry we are able to extract relevant temperatures from samples of various treatment processes. We find no strong evidence for direct correlation between transition temperatures and addition of anti-freeze proteins. We do however note the general trend of our data, suggesting a decrease in T_{g} with addition of AFP, a feature that appears in all comparisons of samples whose differences involve these. Further research is recommended in several areas to further determine the exact behavior of T_{g} and T_{M}

The next step in studying these phenomena lies in the future experiments and research conducted to see what other interesting details exist to be discovered about the molecular effects of such proteins.

References

[1] *Batman & Robin*. URL: https://www.imdb.com/title/tt0118688/quotes/qt0471399 (cit. on p. 1).

[2] Leonard B. Lane. "Freezing Points of Glycerol and its Aqueous Solutions". In: *Industrial and Engineering Chemistry* 17.9 (1925), p. 924. ISSN: 00197866. DOI: 10.1021/ie50189a017 (cit. on pp. 1, 25, 26).

[3] M. D. Ediger, C. A. Angell, and Sidney R. Nagel. "Supercooled Liquids and Glasses". In: *The Journal of Physical Chemistry* 100.31 (1996), pp. 13200–13212 (cit. on pp. 1, 5).

[4] Bo Jakobsen et al. "Thermalization calorimetry: A simple method for investigating glass transition and crystallization of supercooled liquids". In: *AIP Advances* 6.5 (2016). ISSN: 21583226. DOI: 10.1063/1.4952404. arXiv: 1511.09206 (cit. on pp. 1, 7, 8, 24, 25).

[5] Hans Ramløv and Dennis S. Friis. *Antifreeze Proteins : Biochemistry, Molecular Biology and Applications*. Springer, 2020 (cit. on pp. 1, 5).

[6] Johannes Bachler et al. "Glass polymorphism in glycerol-water mixtures: II. Experimental studies". In: *Physical Chemistry Chemical Physics* 18.16 (2016), pp. 11058–11068. ISSN: 14639076. DOI: 10.1039/c5cp08069j (cit. on pp. 1, 25, 26).

[7] Mikkel H. Jensen et al. "Slow rheological mode in glycerol and glycerol-water mixtures". In: (Sept. 2017) (cit. on pp. 1, 25, 26).

[8] Yoshihito Hayashi et al. "Relaxation dynamics in glycerol-water mixtures. 2. Mesoscopic feature in water rich mixtures". In: *Journal of Physical Chemistry B* 109.18 (2005), pp. 9174–9177. ISSN: 15206106. DOI: 10.1021/jp050425d (cit. on pp. 1, 25, 26).

[9] Ivan Popov et al. "The puzzling first-order phase transition in water-glycerol mixtures". In: *Physical Chemistry Chemical Physics* 17.27 (2015), pp. 18063–18071. ISSN: 14639076. DOI: 10.1039/c5cp02851e (cit. on pp. 1, 25, 26).

[10] ZhaoHua Chang, Thomas N. Hansen, and John G. Baust. "The Effect of Antifreeze Protein on the Devitrification of a Cryoprotective System". In: *Cryo-Letters* 12 (1991), pp. 215–226 (cit. on pp. 1, 7).

[11] Rosaria Grasso et al. "Exploring the behaviour of water in glycerol solutions by using delayed luminescence". In: *PLoS ONE* 13 (1 2018) (cit. on p. 2).

[12] Jennifer L. Dashnau et al. "Hydrogen bonding and the cryoprotective properties of glycerol/water mixtures". In: *Journal of Physical Chemistry B* 110 (27 July 2006), pp. 13670–13677 (cit. on p. 2).

[13] Daniel V. Schroeder. *An Introduction to Thermal Physics*. Addison-Wesley, 1999 (cit. on pp. 3–5).

[14] Hans C. Ohanian and John T. Markert. *Physics for Engineers and Scientists*. 3rd ed. W. W. Norton & Company, Inc., 2006 (cit. on pp. 3, 5).

[15] Robert A. Adams and Christopher Essex. *Calculus : a complete course*. 9th ed. Pearson, 2016 (cit. on p. 3).

[16] James A Raymond and Arthur L Devriesf. *Adsorption inhibition as a mechanism of freezing resistance in polar fishes (fish antifreeze/crystal growth inhibition/freezing point depression)*. 1977, pp. 2589–2593 (cit. on p. 5).

[17] Erlend Kristiansen and Karl Erik Zachariassen. "The mechanism by which fish antifreeze proteins cause thermal hysteresis". In: *Cryobiology* 51 (3 2005), pp. 262–280. ISSN: 10902392 (cit. on p. 5).

[18] Dominique Verreault et al. "Ice-binding site of surface-bound type III antifreeze protein partially decoupled from water". In: *Physical Chemistry Chemical Physics* 20 (42 2018), pp. 26926–26933. ISSN: 14639076. DOI: 10.1039/c8cp03382j (cit. on p. 5).

[19] Chen Wang et al. "Structural basis of antifreeze activity of a bacterial multi-domain antifreeze protein". In: *PLoS ONE* 12 (11 Nov. 2017). ISSN: 19326203. DOI: 10.1371/journal.pone.0187169 (cit. on p. 6).

[20] Sandi Brudar and Barbara Hribar-Lee. "Effect of buffer on protein stability in aqueous solutions: A simple protein aggregation model". In: *Journal of Physical Chemistry B* 125 (10 Mar. 2021), pp. 2504–2512. ISSN: 15205207. DOI: 10.1021/acs.jpcb.0c10339 (cit. on p. 11).

[21] Kalim Deshmukh. *From: Orthodontic Applications of Biomaterials*. 2017 (cit. on p. 26).